Effects of Immune Response and Time Delays in Models of Acute Myeloid Leukaemia

Weigang Sun (mawgsun@gmail.com)
Hangzhou Dianzi University https://orcid.org/0000-0001-8699-5392
Lei Yang
Hangzhou Dianzi University
Min Luo
Hangzhou Dianzi University

Research Article

Keywords: Acute myeloid leukaemia, Immune response, Time delay, Bifurcation

Posted Date: November 16th, 2021

DOI: https://doi.org/10.21203/rs.3.rs-981651/v1

Noname manuscript No.
(will be inserted by the editor)

Effects of immune response and time delays in models of acute myeloid leukaemia

Weigang Sun* · **Lei Yang** · **Min Luo**

Received: date / Accepted: date

Abstract In this paper, we propose a general acute myeloid leukaemia (AML) model and introduce an immune response and time delays into this model to investigate their effects on the dynamics. Based on the existence, stability and local bifurcation of three types of equilibria, we show that the immune response is a best strategy for the control of the AML on the condition that the rates of proliferation and differentiation of the hematopoietic lineage exceed a threshold. In particular, a powerful immune response leads to bi-stability of the steady states, and a stronger response wipes out all the leukaemia cells. In addition, we further reveal that the time delays existing in the feedback regulation and immune response process induce a series of oscillations around the steady state, which shows that the leukaemia cells can hardly be eliminated. Our work in this paper aims to investigate the complex dynamics of this AML model with the immune response and time delays on the basis of mathematical models and numerical simulations, which may provide a theoretical guidance for the treatments of the AML.

Keywords Acute myeloid leukaemia · Immune response · Time delay · Bifurcation

1 Introduction

Acute myeloid leukaemia (AML) is a blood cancer which is aroused by the malignant clone of hematopoietic stem cells or hematopoietic progenitor cells. Those anomalous cells mutate as leukaemia original cells, inhibit the normal proliferation and differentiation of hematopoietic cells, and destroy the hematopoietic function of the bone marrow[1]. AML is a common myeloid disease with a great mortality rate and has attracted considerable attention in the clinical pathogenesis and treatment [2]. Based on a lot of experiments for the mouse, the leukaemia original cells, i.e., the leukaemia stem cells, have been found and defined [3,4], which shows a new way to the diagnosis and treatment of the AML [5,6]. With the development of molecular biology, there are more and more treatments of the AML,

W. Sun · L. Yang · M. Luo
School of Sciences, Hangzhou Dianzi University, Hangzhou 310018, China
E-mail: mawgsun@gmail.com

such as transplantation of bone marrow stem cells [7], targeted chemotherapy [8], combination chemotherapy [9] and resonance chemotherapy [10, 11]. However, the treatments face a greater challenge because of the complicated interactions among the cells in the bone marrow. Therefore, it is of interest to model these interactions in the mathematical manner to provide a theoretical guidance to the AML [12–14].

There are two multi-stage lineages in the bone marrow, i.e., hematopoietic lineage and leukaemia lineage. The hematopoietic stem cell (HSC) of the hematopoietic lineage is multipotent, which maintains the population by proliferation and differentiates into different mature cells. The hematopoietic progenitor cell (HPC) is mono-potent and has the ability to proliferate and differentiate into the functional cells (e.g., red blood cells and platelets). The leukaemia stem cell (LSC) in the leukaemia lineage has a similar feature with the HPC and proliferates into itself and differentiates into the leukaemia cells. On the basis of cancer stem cells hypothesis [15], it is of significance to investigate the characteristics (e.g., proliferation, differentiation and death) of the cells in the hematopoietic lineage and the leukaemia lineage, and interactions (e.g., competition and feedback) between them [16–18].

Presently mathematical models have been proposed to characterize the competition, feedback and immune response in the AML model [19]. Goardon et al. found that the LSC shares more characteristic with the HPC [20, 21]. The LSC and HPC can proliferate and differentiate into only one type of cells by consuming the energy in the bone marrow, but they have to compete with each other, which results in the coupling between the hematopoietic lineage and leukaemia lineage, further leads to complex dynamics of the system [22–24]. Ignacio et al. showed that a key of the carcinogenic process is that the proliferation and differentiation of the LSC break away the inhibition feedback from terminally differentiated cells in the leukaemia lineage [25]. To control the output of multi-stage cell lineages, Lander et al. studied different types of feedback configurations, feedback sensitivities [26, 27] in the linages. For the treatment and prevention of the AML, Crowell et al. regulated the feedback's strength among of the HSC, HPC and LSC [28, 29]. To derive optimal control strategies, Sharp et al. introduced immune function into AML model and showed the effectiveness of treatment by improving the strength of immune response [30].

In biological systems, time delay plays an important role in producing complex dynamics, small time delays often are harmless while larger delays lead to oscillations through a Hopf bifurcation [31–33]. Kim et al. studied the delay effects on the asymptotic stability in modeling the post-transplantation dynamics of the immune response to chronic myelogenous leukemia [34]. In our previous work, the introduced delays induce the Hopf rotation in a time-delayed three-gene auto-regulated and mutually-repressed core genetic regulation network [35]. Inspired by the above-mentioned discussions, we introduce time delays into an AML model characterizing the delays during the feedback regulations in the hematopoietic lineage and the immune response in the leukaemia lineage. We provide a lot of mathematical analysis of the existence, stability and local bifurcation of the steady states of the studied model with an immune response and time delays.

The remainder of this paper is organized as follows. In Sect. 2, we introduce an immune response and time delays into an AML model. Section 3 provides the analysis of the existence, stability and local bifurcation of three types of steady states for the non-delayed model. In Sect. 4, we study the counterparts of the model with time delays and compare them with the non-delayed model. Finally, conclusions are given in Sect. 5.

2 Model formulation

Crowell et al. proposed a classical acute myeloid leukaemia (AML) model [28], which is given by

$$\begin{aligned}
\frac{dS}{dt} &= \rho_S S(K_1 - Z_1) - \delta_S S,\\
\frac{dA}{dt} &= \delta_S S + \rho_A A(K_2 - Z_2) - \delta_A A,\\
\frac{dD}{dt} &= \delta_A A - \mu_D D,\\
\frac{dL}{dt} &= \rho_L L(K_2 - Z_2) - \delta_L L,\\
\frac{dT}{dt} &= \delta_L L - \mu_T T,
\end{aligned} \tag{1}$$

where S, A, D, L, T represent haematopoietic stem cells (HSCs), haematopoietic progenitor cells (HPCs), terminally differentiated blood cells, leukaemia stem cells (LSCs) and fully differentiated leukaemia cells, respectively. The quantities $0 < \rho_S, \rho_A, \rho_L < 1$ and $0 < \delta_S, \delta_A, \delta_L < 1$ are the proliferation rates and differentiation rates of HSCs (S), HPCs (A) and LSCs (L). $0 < \mu_D < 1$ and $0 < \mu_T < 1$ are the death rates of terminally differentiated blood cells (D) and leukaemia cells (T). K_1 and K_2 are the population sizes of cells within the bone marrow which determine the carrying capacities. In the following studies, we scale the populations sizes $K_1 = K_2 = 1$. $Z_1 \equiv S$ and $Z_2 \equiv A + L$ are the total niche size, where A and L are coupled because of the competition between LSCs (L) and HPCs (A), which is resulted by the hypothesis that LSCs (L) and HPCs (A) occupy the same niche in the bone marrow [9,28,36].

On the basis of the model (1), Sharp et al. introduced an immune response to apply the optimal control [30]. The feature of this model considers a small population of leukemia may be overcome by the healthy cells without the intervention [19]. Then, the model (1) is written as

$$\begin{aligned}
\frac{dS}{dt} &= \rho_S S(K_1 - Z_1) - \delta_S S,\\
\frac{dA}{dt} &= \delta_S S + \rho_A A(K_2 - Z_2) - \delta_A A,\\
\frac{dD}{dt} &= \delta_A A - \mu_D D,\\
\frac{dL}{dt} &= \rho_L L(K_2 - Z_2) - \delta_L L - \frac{\alpha L}{\gamma + L},\\
\frac{dT}{dt} &= \delta_L L - \mu_T T,
\end{aligned} \tag{2}$$

where $\alpha > 0$ and $\gamma > 0$ are the parameters controlling the intensity of immune response.

To investigate the effects of feedback regulation, Jiao et al. introduced the Hill function to characterize the feedback regulation in the haematopoietic lineage [29]. The model is

described in the form below:

$$\begin{aligned}
\frac{dS}{dt} &= \big[p_1(D)(K_1-Z_1)-(1-p_1(D))\big]v_1(D)S,\\
\frac{dA}{dt} &= 2(1-p_1(D))v_1(D)S+\big[p_2(D)(K_2-Z_2)-(1-p_2(D))\big]v_2(D)A,\\
\frac{dD}{dt} &= 2(1-p_2(D))v_2(D)A-\mu_D D,\\
\frac{dL}{dt} &= \big[p_{30}(K_2-Z_2)-(1-p_{30})\big]v_{30}L,\\
\frac{dT}{dt} &= 2(1-p_{30})v_{30}L-\mu_T T,
\end{aligned} \tag{3}$$

where $p_i(D)=\frac{p_{i0}}{1+g_iD^n}, v_i(D)=\frac{v_{i0}}{1+h_iD^n}, i=1,2$. n is the Hill exponent. The feedback coefficients are $g_i,h_i\geq 0, i=1,2$. p_{i0} and $v_{i0}, (i=1,2,3)$ are the maximal proliferation rates and division rates of S,A,L. Based on the biological significance and mathematical principles, it is assumed that $0<p_{i0}<1$, $v_{i0}>0$.

Based on the models (2) and (3), we propose a new model with the immune response and feedback regulation to investigate the effect of intensity of the immune response on the dynamics. The model reads as

$$\begin{aligned}
\frac{dS}{dt} &= \big[p_1(D)(K_1-Z_1)-(1-p_1(D))\big]v_1(D)S,\\
\frac{dA}{dt} &= 2(1-p_1(D))v_1(D)S+\big[p_2(D)(K_2-Z_2)-(1-p_2(D))\big]v_2(D)A,\\
\frac{dD}{dt} &= 2(1-p_2(D))v_2(D)A-\mu_D D,\\
\frac{dL}{dt} &= \big[p_{30}(K_2-Z_2)-(1-p_{30})\big]v_{30}L-\frac{\alpha L}{\gamma+L},\\
\frac{dT}{dt} &= 2(1-p_{30})v_{30}L-\mu_T T.
\end{aligned} \tag{4}$$

In addition, there also exist time delays between the feedback regulation and immune process. Therefore, we introduce $\tau_1>0$, $\tau_2>0$ to describe the time lags during feedback processes from terminally differentiated blood cells (D) to HSCs (S) and HPCs (A). In addition, the time delay $\tau_3>0$ shows the lag during the immune response of LSCs (L). Then, the model (4) becomes

$$\begin{aligned}
\frac{dS}{dt} &= \big[p_1(D(t-\tau_1))(K_1-Z_1)-(1-p_1(D(t-\tau_1)))\big]v_1(D(t-\tau_1))S,\\
\frac{dA}{dt} &= 2(1-p_1(D(t-\tau_1)))v_1(D(t-\tau_1))S+\big[p_2(D(t-\tau_2))(K_2-Z_2)\\
&\quad -(1-p_2(D(t-\tau_2)))\big]v_2(D(t-\tau_2))A,\\
\frac{dD}{dt} &= 2(1-p_2(D(t-\tau_2)))v_2(D(t-\tau_2))A-\mu_D D,\\
\frac{dL}{dt} &= \big[p_{30}(K_2-Z_2)-(1-p_{30})\big]v_{30}L-\frac{\alpha L(t-\tau_3)}{\gamma+L(t-\tau_3)},\\
\frac{dT}{dt} &= 2(1-p_{30})v_{30}L-\mu_T T.
\end{aligned} \tag{5}$$

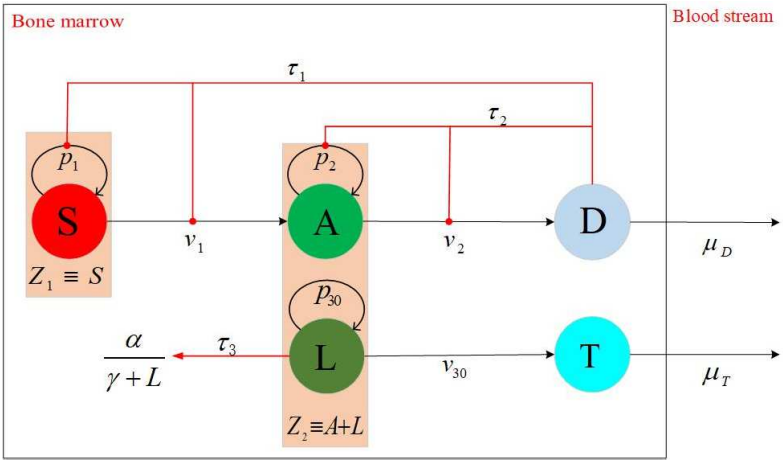

Fig. 1 Schematic diagram of leukemogenesis and haematopoietic stem cell lineages regarding immune response and time delays. The black arrows above S, A and L represent their proliferation process, the black arrows from S to A, A to D, and L to T denote the division process. The red dot-head arrows indicate the feedback inhibitions to the proliferation and division from the cell (D) to S and A. τ_1 and τ_2 denote the time delays during the inhibition processes. τ_3 is the delay during the immune response of L and $\frac{\alpha}{\gamma+L}$ is the immune response.

The schematic diagram introducing the immune response and time delays is shown in Fig. 1, the definitions and basal values for all the parameters are given in the Appendix B.

3 Effects of intensity of immune response

In this section, we discuss the existence, stability and local bifurcations of positive equilibria of the model (4) with the varying of the intensity of immune response to investigate the influence of immune response.

3.1 Existence of the equilibria

It is obvious that the origin is a trivial equilibrium of the system (4), which should be globally stable based on the biological significance and theoretical analysis. Similar with the analysis in [29], we divide the equilibria into three types, denoted by $E_l(0,0,0,L_l^*,T_l^*)$, $E_h(S_h^*,A_h^*,D_h^*,0,0)$, and $E_c(S_c^*,A_c^*,D_c^*,L_c^*,T_c^*)$, where E_l is a purely leukemic steady state with $S=A=D=0$, which means that there are only LSCs (L) and terminally differentiated leukaemia cells (T). E_h is a healthy steady state when there are only healthy cells in the bone marrow, i.e., $L=T=0$. E_c is a coexisting steady state when both the healthy cells (S,A,D) and the leukaemia cells (L,T) coexist in the bone marrow. Firstly, we discuss the existence of these three types of equilibria to investigate the effect of immune response on the existence.

Theorem 1 *There are at most two purely leukaemia steady states E_l according to the values of p_{30} and α.*

Proof It is from (4) that

$$L_l^{*2} + L_l^*(\gamma - (2 - \frac{1}{p_{30}})) - (2 - \frac{1}{p_{30}})\gamma + \frac{\alpha}{p_{30}v_{30}} = 0. \tag{6}$$

The number of positive roots of Eq. (6) depends on the values of Δ, where $\Delta = (\gamma + (2 - \frac{1}{p_{30}}))^2 - 4\frac{\alpha}{p_{30}v_{30}}$. When $\Delta > 0$ and $\alpha > p_{30}v_{30}(2 - \frac{1}{p_{30}})\gamma$, $\gamma < (2 - \frac{1}{p_{30}})$, the model (4) has two positive roots $E_{l1}(0,0,0,L_{l1}^*,T_{l1}^*)$ and $E_{l2}(0,0,0,L_{l2}^*,T_{l2}^*)$, where $L_{l1}^* = \frac{1}{2}\big((2 - \frac{1}{p_{30}}) - \gamma + \sqrt{\Delta}\big)$, $L_{l2}^* = \frac{1}{2}\big((2 - \frac{1}{p_{30}}) - \gamma - \sqrt{\Delta}\big)$, $T_{l1}^* = \frac{2(1-p_{30})v_{30}}{\mu_T}L_{l1}^*$ and $T_{l2}^* = \frac{2(1-p_{30})v_{30}}{\mu_T}L_{l2}^*$. On the other hand, when $\Delta > 0$ and $\alpha < p_{30}v_{30}(2 - \frac{1}{p_{30}})\gamma$ or $\Delta = 0$ and $\gamma < (2 - \frac{1}{p_{30}})$, the model (4) has only one purely leukemic steady state $E_l(0,0,0,L_{l1}^*,T_{l1}^*)$. ■

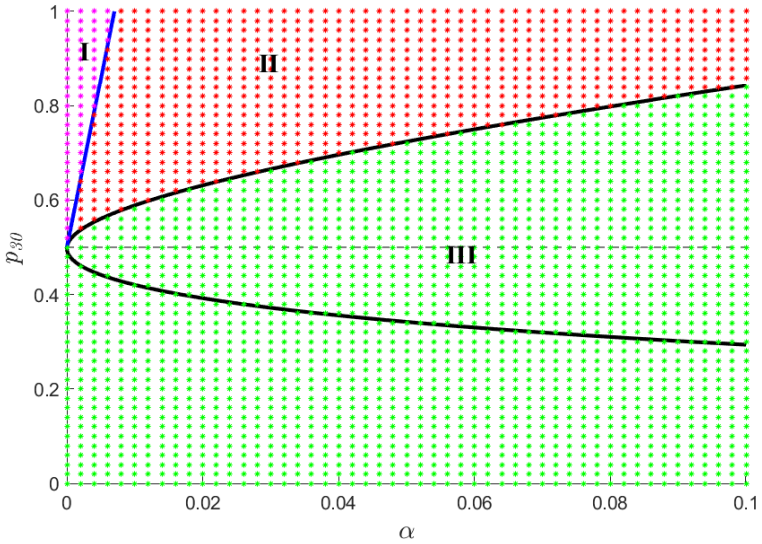

Fig. 2 The number of purely leukaemia steady state E_l is determined by the values of p_{30} and α. The black and blue lines represent $\Delta = 0$ and $\alpha = p_{30}v_{30}(2 - 1/p_{30})\gamma$, respectively. The symbol II (I, III) means that system (4) has 2(1,0) steady states E_l. By adjusting the appropriate immune response α and differentiation probability p_{30}, there will not exist purely leukaemia steady state.

As shown in Fig. 2, there is no purely leukaemia steady state (III) under the condition $\alpha > p_{30}v_{30}(2 - 1/p_{30})\gamma$.

Theorem 2 *There exists a healthy steady state E_h when $p_{10} > 0.5$ and $\sum_{i=1}^{6} a_i > 0$.*

Proof For the healthy steady state E_h, $S_h^* = 2 - \frac{1}{p_1(D_h^*)}$, $A_h^* = \frac{\mu_D D_h^*}{2(1-p_2(D_h^*))v_2(D_h^*)}$, and D_h^* is the root of the following equation:

$$F_0(D) \equiv a_6D^6 + a_5D^5 + a_4D^4 + a_3D^3 + a_2D^2 + a_1D + a_0 = 0. \tag{7}$$

If $p_{10} > 0.5$, it gives $a_0 < 0$, i.e. $F_0(0) < 0$. When $F_0(1) = \sum_{i=1}^{6} a_i > 0$, there exists a positive root of Eq. (7), which is located in the interval $(0,1)$. ■

According to Eq. (7), the existence of E_h is mainly determined by p_{10} and p_{20}, not related to the immune response (α) and the proliferation rate p_{30}. When the rates p_{10} and p_{20} reach a threshold, it supports that the HPCs compete with the LSCs, which means that increasing the intensity of the immune response inhibits the leukaemia stem cells.

Theorem 3 *There are at most two coexisting steady states E_c, which is determined by the equation $G(L,D) - H(L,D) = 0$.*

Proof From the system (4), the coexisting steady state E_c satisfies the following equations: $S = 2 - \frac{1}{p_1(D)}, A = \frac{\mu_D D}{2(1-p_2(D))v_2(D)}, T = \frac{2(1-p_{30})v_{30}L}{\mu_T}, G(L,D) = 0, H(L,D) = 0$, where

$$\begin{aligned}
G(L,D) =& 2p_{10}p_{20}(1+g_1D)(1+g_2D-p_{20})(1+h_1D)v_{20}\mu_D DL \\
&- 8(1+g_2D-p_{20})^2v_{10}v_{20}(3p_{10}(1+g_1D) - 2p_{10}^2 - (1+g_1D)^2) \\
&- \mu_D D p_{10}\big[(1+h_1D)(1+g_1D)(1+g_2D-p_{20})4p_{20}v_{20} \\
&- (1+g_1D)(1+g_2D)(1+h_1D)(1+h_2D)\mu_D D p_{20} \\
&- 2(1+g_1D)(1+g_2D)(1+h_1D)(1+g_2D-p_{20})v_{20}\big], \\
H(L,D) =& -2p_{30}v_{20}v_{30}(1+g_2D-p_{20})L^2 + \big(2v_{20}(1+g_2D-p_{20})(2p_{30}-1-p_{30}\gamma) \\
&- p_{30}\mu_D D(1+g_2D)(1+h_2D)\big)v_{30}L + 2v_{20}(1+g_2D-p_{20})\big(v_{30}\gamma(2p_{30}-1) - \alpha\big) \\
&- p_{30}v_{30}\gamma\mu_D D(1+g_2D)(1+h_2D).
\end{aligned}$$

The number of coexisting steady state is same as the number of intersections between the curves $H(L,D) = 0$ and $G(L,D) = 0$. ■

There exists one or two coexisting steady states when the proliferation rate p_{30} of the LSCs is bigger than the rate p_{10} of the HSCs and the rate p_{20} of the HPCs, see Fig. 3.

3.2 Stability of the equilibria

In this subsection, we discuss the stability of the equilibria E_l, E_h and E_c and bifurcation mechanisms regarding to the intensity parameter α of the immune response.

The Jacobian matrix $J(S,A,D,L,T)$ of the system (4) is given by:

$$J(S,A,D,L,T) = \begin{pmatrix}
f_{1S} & 0 & f_{1D} & 0 & 0 \\
f_{2S} & f_{2A} & f_{2D} & f_{2L} & 0 \\
0 & f_{3A} & f_{3D} & 0 & 0 \\
0 & f_{4A} & 0 & f_{4L} & 0 \\
0 & 0 & 0 & f_{5L} & f_{5T}
\end{pmatrix},$$

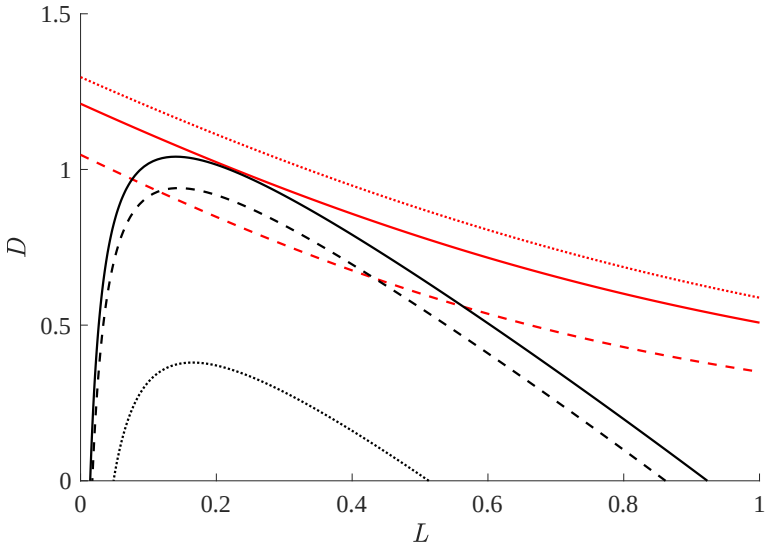

Fig. 3 The existence of coexisting steady state (E_c). The number of intersections of the curves $G(L,D)=0$ (red) and $H(L,D)=0$ (black) corresponds to the number of coexisting steady state (E_c). If $p_{10}=0.55, p_{30}=0.9$ (discontinuous line), $p_{10}=0.6, p_{30}=0.95$ (continuous line) and $p_{10}=0.65, p_{30}=0.7$ (dot line), the system (4) will have two or one or zero coexisting steady state.

where

$$
\begin{aligned}
&f_{1S}=\big[2p_1-1-2p_1S\big]v_1, f_{1D}=S(2-S)v_1p_{1D}+\big[2p_1-p_1S-1\big]v_{1D}S,\\
&f_{2S}=2(1-p_1)v_1, f_{2A}=\big[p_2(2-2A-L)-1\big]v_2, f_{2L}=-p_2v_2A,\\
&f_{2D}=2S(1-p_1)v_{1D}-2Sp_{1D}v_1+\big[p_2(2-A-L)-1\big]v_{2D}A+(2-A-L)p_{2D}v_2A,\\
&f_{3A}=2(1-p_2)v_2, f_{3D}=2(1-p_2)v_{2D}A-2p_{2D}v_2A-\mu_D,\\
&f_{4A}=-p_{30}v_{30}L, f_{4L}=\big[2p_{30}-p_{30}A-2p_{30}L-1\big]v_{30}-\frac{\alpha\gamma}{(\gamma+L)^2},\\
&f_{5L}=2(1-p_{30})v_{30}, f_{5T}=-\mu_T,
\end{aligned}
$$

and

$$
p_{iD}=-\frac{np_{i0}g_iD^{n-1}}{(1+g_iD^n)^2},\quad v_{iD}=-\frac{nv_{i0}h_iD^{n-1}}{(1+h_iD^n)^2},\quad i=1,2.
$$

Theorem 4 *The purely leukemic steady state E_l is locally stable when $p_{10}<0.5$, $p_{20}<\frac{1}{2-L_l^*}$ and $p_{30}<\frac{1}{2(1-L_l^*)}\big(\frac{\alpha\gamma}{(\gamma+L_l^*)^2v_{30}}+1\big)$.*

Proof The Jacobian matrix at the state E_l is

$$J(E_l)=\begin{pmatrix}(2p_{10}-1)v_{10} & 0 & 0 & 0 & 0\\ 2(1-p_{10})v_{10} & \big(p_{20}(2-L_l^*)-1\big)v_{20} & 0 & 0 & 0\\ 0 & 2(1-p_{20})v_{20} & -\mu_D & 0 & 0\\ 0 & -p_{30}v_{30}L_l^* & 0 & (2p_{30}(1-L_l^*)-1)v_{30}-\frac{\alpha\gamma}{(\gamma+L_l^*)^2} & 0\\ 0 & 0 & 0 & 2(1-p_{30})v_{30} & -\mu_T\end{pmatrix}.$$

Then, the eigenvalues are as follows:

$$\begin{aligned}&\lambda_{l1}=(2p_{10}-1)v_{10},\quad \lambda_{l2}=\big(p_{20}(2-L_l^*)-1\big)v_{20},\quad \lambda_{l3}=-\mu_D,\\ &\lambda_{l4}=(2p_{30}-2p_{30}L_l^*-1)v_{30}-\frac{\alpha\gamma}{(\gamma+L_l^*)^2},\quad \lambda_{l5}=-\mu_T.\end{aligned}\tag{8}$$

When $\lambda_{l1}=(2p_{10}-1)v_{10}<0$, $\lambda_{l2}=\big(p_{20}(2-L_l^*)-1\big)v_{20}<0$ and $\lambda_{l4}=(2p_{30}-2p_{30}L_l^*-1)v_{30}-\frac{\alpha\gamma}{(\gamma+L_l^*)^2}<0$, the steady state E_l is stable. ■

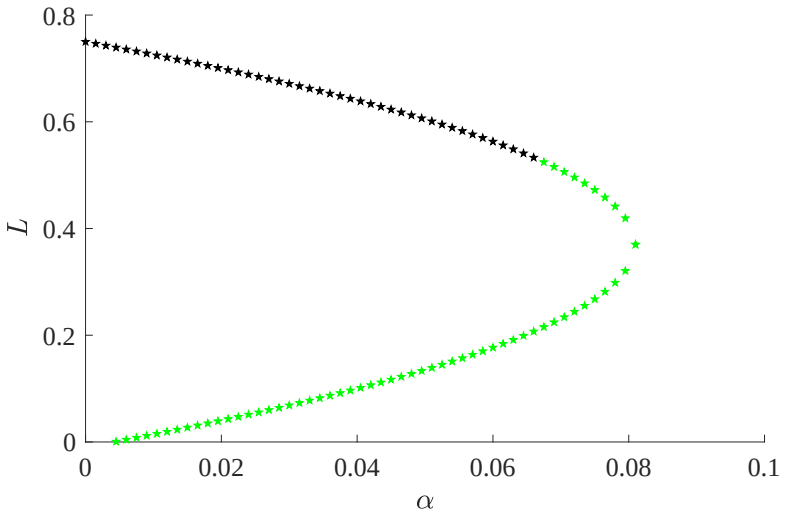

Fig. 4 The stability of E_l versus α with $p_{10}=0.45$,$p_{20}=0.68$, $p_{30}=0.8$. Black (green) stars denote the stable (unstable) equilibria E_l.

As shown in Fig. 4, there are two purely leukaemia steady states $E_{l1}(0,0,0,0.71295,0.66542)$ and $E_{l2}(0,0,0,0.027051,0.025247)$ when $p_{10}=0.45$, $p_{20}=0.68$, $p_{30}=0.8$. According to Theorem 4, it follows that E_{l1} is stable and E_{l2} is unstable. Since only the eigenvalue λ_{l4} is related to the intensity α, the stable equilibrium becomes unstable with the increasing values of the intensity. According to the above analysis, increasing the strength of immune response can transform a stable steady state E_l into an unstable one, which shows it is an efficient form to treat the AML. On the other hand, we need to change the states of system (4) into the healthy or coexisting steady states to prevent the relapse of the AML.

Theorem 5 *The steady states E_c and E_h are locally stable under the conditions $H_i > 0$, $i = 1, \cdots, 5$.*

Proof The characteristic equation is

$$\begin{aligned}\Delta(\lambda) =&(\lambda - f_{5T})\Big[(\lambda - f_{1S})\big[(\lambda - f_{2A})(\lambda - f_{3D})(\lambda - f_{4L}) - f_{2D}f_{3A}(\lambda - f_{4L})\\ &- f_{2L}(\lambda - f_{3D})f_{4A}\big] - f_{1D}f_{2S}f_{3A}(\lambda - f_{4L})\Big], \\ =&\lambda^5 + A_4\lambda^4 + A_3\lambda^3 + A_2\lambda^2 + A_1\lambda + A_0.\end{aligned} \tag{9}$$

Based on the Routh-Hurwize stability criterion, all the roots of characteristic Eq. (9) have negative real parts if and only if

$$\begin{aligned}&H_1 = A_4 > 0,\\ &H_2 = A_4A_3 - A_2 > 0,\\ &H_3 = A_4(A_3A_2 - A_1A_4) - (A_2^2 - A_0A_4) > 0,\\ &H_4 = A_4\big(A_3(A_1A_2 - A_0A_3) - A_1(A_1A_4 - A_0)\big) - A_2(A_1A_2 - A_0A_3) + A_0(A_1A_4 - A_0) > 0,\\ &H_5 = A_0H_4 > 0.\end{aligned}$$

Therefore, the coexisting steady state E_c and healthy steady state E_h are locally stable when the conditions $H_i > 0, (i = 1, \cdots, 5)$ hold. ■

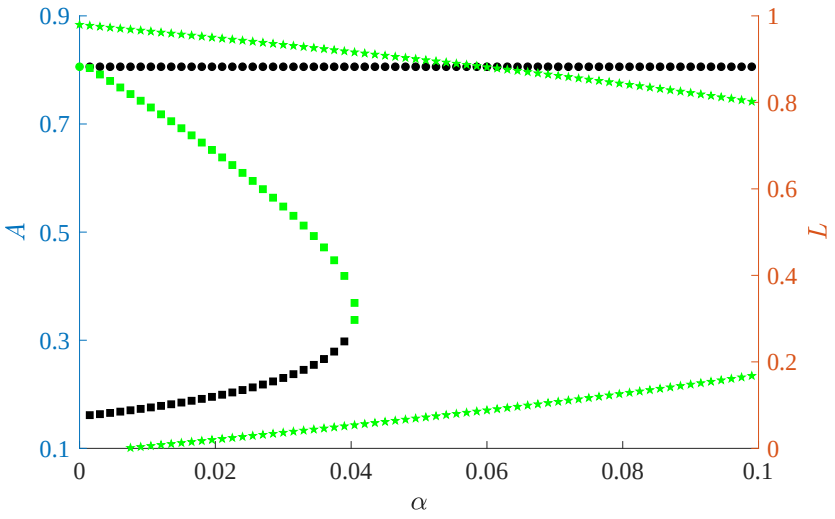

Fig. 5 The stability of three types of equilibria against α with $p_{10} = 0.51, p_{20} = 0.85, p_{30} = 0.98$. Black (green) points represent stable (unstable) equilibria. Square, round dot and star signs denote the states E_c,E_h and E_l, respectively.

In Fig. 5, when the immune response is very weak ($\alpha \to 0$), there have no stable coexisting and healthy equilibria. With an increase of the intensity of immune response, there

appears a bi-stability state, even a mono-stability state, which shows that the leukaemia cells will be eliminated by a powerful immune response.

3.3 Local bifurcation

In this subsection, we discuss the effects of the intensity of immune response to the local bifurcation around the three types of equilibria.

3.3.1 Transcritical bifurcation

Transcritical bifurcation is characterized by the exchanging of stability of two equilibria. In this bifurcation,two equilibria cross with each other and the stable equilibrium lose its stability and the unstable one become stable. Transcritical bifurcation may take place at a non-hyperbolic equilibrium point of the system if the Jacobian matrix at the equilibrium has a simple zero eigenvalue, we firstly consider the transcritical bifurcation around the healthy steady state $E_h(S_h^*, A_h^*, D_h^*, 0, 0)$, and regard the immune response α as a bifurcation parameter.

Theorem 6 *The system (4) undergoes a transcritical bifurcation around the healthy steady state E_h at the critical value $\alpha_{[Th]} = \gamma v_{30}\left[2p_{30} - p_{30}A_h^* - 1\right]$, and around the purely leukaemia steady state E_l at $\alpha_{[Tl]}$, where $\alpha_{[Tl]}$ is the root of $L_l^*(\alpha) = 2 - \frac{1}{p_{20}}$.*

Proof For $\alpha = \alpha_{[Th]}$, the Jacobian matrix is

$$J(E_h, \alpha_{[Th]}) = \begin{pmatrix} f_{1S} & 0 & f_{1D} & 0 & 0 \\ f_{2S} & f_{2A}|_{L=0} & f_{2D}|_{L=0} & f_{2L} & 0 \\ 0 & f_{3A} & f_{3D} & 0 & 0 \\ 0 & 0 & 0 & 0 & 0 \\ 0 & 0 & 0 & f_{5L} & f_{5T} \end{pmatrix}.$$

Then, its characteristic equation is

$$\Delta_{[Th]}(\lambda) = \lambda(\lambda - f_{5T})\Big[(\lambda - f_{1S})\big[(\lambda - f_{2A})(\lambda - f_{3D}) - f_{2D}f_{3A}\big] - f_{1D}f_{2S}f_{3A}\Big]. \quad (10)$$

Clearly, the equation (10) has a simple zero eigenvalue at the threshold point $\alpha_{[Th]} = \gamma v_{30}\big[2p_{30} - p_{30}A_h^* - 1\big]$. The eigenvectors of $J(E_h, \alpha_{[Th]})$ and $J(E_h, \alpha_{[Th]})^T$ corresponding to the zero eigenvalue are denoted by $V_{[Th]} = \big(1 \ v_{2h} \ v_{3h} \ v_{4h} \ v_{5h}\big)^T$ and $W_{[Th]} = \big(0 \ 0 \ 0 \ 1 \ 0\big)^T$, where

$$\begin{aligned} v_{2h} &= \frac{f_{1S}f_{3D}}{f_{1D}f_{3A}}|_{E_h}, \\ v_{3h} &= -\frac{f_{1S}}{f_{1D}}|_{E_h}, \\ v_{4h} &= -\frac{1}{f_{2L}}\big[f_{2S} + \frac{f_{1S}f_{2A}f_{3D}}{f_{1D}f_{3A}} + \frac{f_{1S}f_{2D}}{f_{1D}}\big]|_{E_h}, \\ v_{5h} &= -\frac{f_{5L}}{f_{2L}f_{5T}}\big[f_{2S} + \frac{f_{1S}f_{2A}f_{3D}}{f_{1D}f_{3A}} + \frac{f_{1S}f_{2D}}{f_{1D}}\big]|_{E_h}. \end{aligned}$$

Therefore, the transversality conditions for the transcritical bifurcation are

$$\Delta_{1h} = W_{[Th]}^T \left[F_\alpha(E_h, \alpha_{[Th]}) \right] = 0,$$
$$\Delta_{2h} = W_{[Th]}^T \left[DF_\alpha(E_h, \alpha_{[Th]}) V_{[Th]} \right] = -\frac{v_{4h}}{\gamma} \neq 0,$$
$$\Delta_{3h} = W_{[Th]}^T \left[D^2 F(E_h, \alpha_{[Th]})(V_{[Th]}, V_{[Th]}) \right] = -2p_{30}v_{30}v_{2h}v_{4h} + v_{4h}^2 \left(-2p_{30}v_{30} + \frac{2\alpha_{[Th]}}{\gamma^2} \right) \neq 0.$$

Based on Sotomayor's theorem for transcritical bifurcation [37], we conclude that the system (4) experiences a transcritical bifurcation around E_h at the threshold $\alpha_{[Th]}$. The proof of the bifurcation at E_l is similar with the above-mentioned proof, and it is omitted. ■

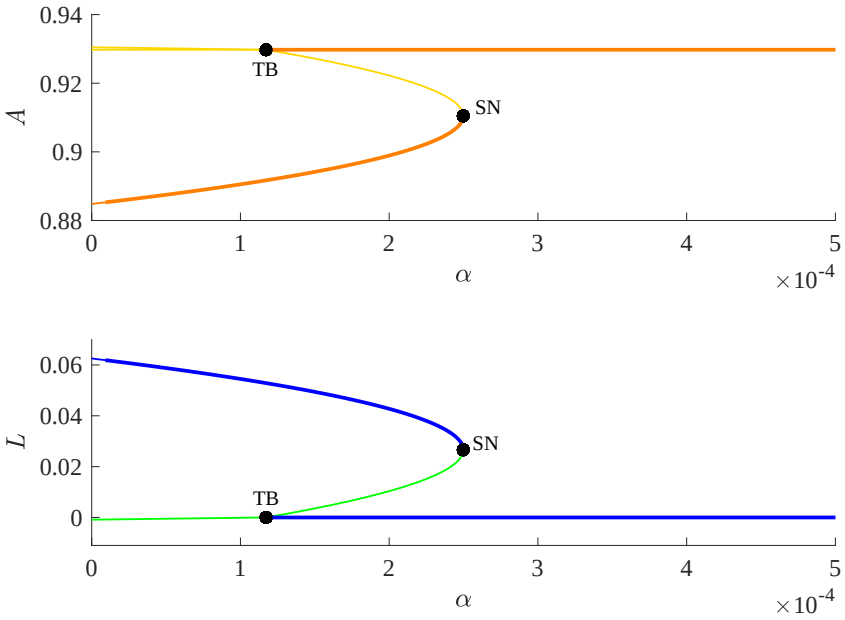

Fig. 6 The bifurcation diagram with respect to A, L and α. The system undergoes a transcritical bifurcation (TB) around the healthy steady state E_h (horizontal line) at $\alpha_{[Th]} = 0.000117$ and a saddle-node bifurcation (SN) around the coexisting steady state E_c (curve) at $\alpha_{[SNc]} = 0.00025$ with $p_{20} = 0.75$, $p30 = 0.95$ and $\mu_D = 0.365$.

The system (4) has a stable healthy steady state $E_h(0.42047, 0.92976, 0.8898, 0, 0)$ with $p_{20} = 0.75$, $p_{30} = 0.95$ and $\mu_D = 0.365$. Then, the threshold is $\alpha_{[Th]} = 0.000117$, which is consistent with the value in Fig. 6. After the transcritical bifurcation, the healthy steady state becomes stable, and the stable coexisting steady state E_c loses its stability. In addition, the state E_c has no biological significance because of the negative population of leukaemia cells. In the same way, the theoretical value $L(\alpha_{[Tl]}) = 2 - 1/p_{20} = 0.5294$ with $\alpha = 0.0665$ and $p_{10} = 0.45$ approximates the numerical value $L = 0.5294122$, see Fig. 7.

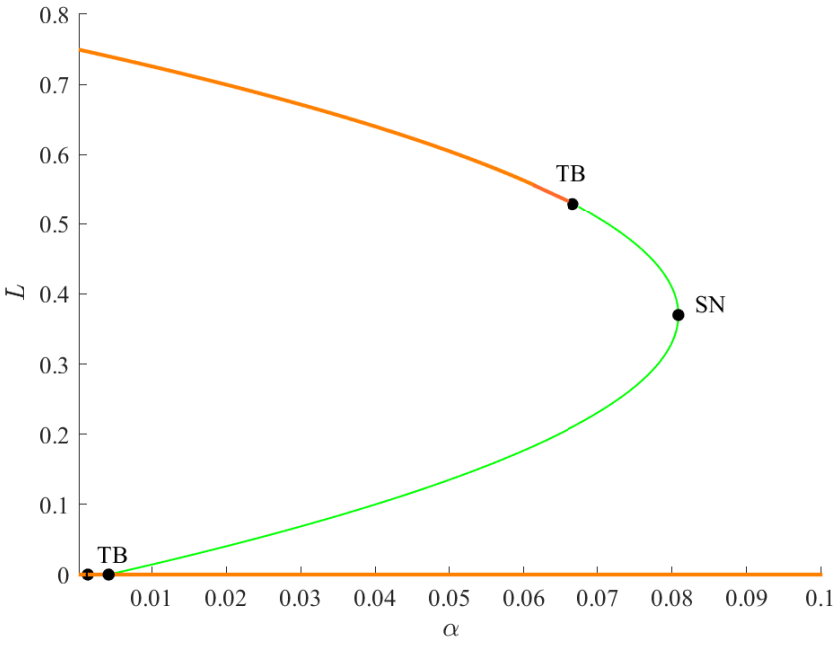

Fig. 7 The bifurcation diagram between L and α. There are two purely leukaemia steady states E_l, one is a stable node and another is an unstable saddle when $p_{10} = 0.45$. There is a saddle-node bifurcation around the unstable E_l at the threshold $\alpha_{[SNl]} = 0.08085$, and a transcritical bifurcation around the stable E_l at $\alpha_{[Tl]} = 0.0665$, a transcritical bifurcation around E_h at $\alpha_{[Th]} = 0.001647$.

3.3.2 Hopf bifurcation

Theorem 7 *If the transversality condition* $\left[\frac{d}{d\alpha}\left(Re(\lambda(\alpha))\right)\right]_{\alpha=\alpha_{[Hc]}} \neq 0$ *holds, the system (4) undergoes a Hopf bifurcation around the coexisting steady state* E_c *at the threshold* $\alpha = \alpha_{[Hc]}$.

Proof Suppose $\lambda = \pm i\omega(\alpha_{[Hc]})$ $(\omega(\alpha_{[Hc]}) > 0)$ is a pair of eigenvalues of the characteristic equation: $\lambda^5 + A_4(\alpha)\lambda^4 + A_3(\alpha)\lambda^3 + A_2(\alpha)\lambda^2 + A_1(\alpha)\lambda + A_0(\alpha) = 0$ with $\alpha = \alpha_{[Hc]}$. It follows that

$$\begin{cases} \omega^5 - A_3(\alpha_{[Hc]})\omega^3 + A_1(\alpha_{[Hc]})\omega = 0, \\ A_4(\alpha_{[Hc]})\omega^4 - A_2(\alpha_{[Hc]})\omega^2 + A_0(\alpha_{[Hc]}) = 0. \end{cases}$$

Let $v = \omega^2$, then

$$v = \omega^2 = \sqrt{\frac{A_1(\alpha_{[Hc]})A_4(\alpha_{[Hc]}) - A_0(\alpha_{[Hc]})}{A_3(\alpha_{[Hc]})A_4(\alpha_{[Hc]}) - A_2(\alpha_{[Hc]})}}.$$

Substituting $\lambda = p(\alpha) \pm iq(\alpha)$ into the characteristic equation yields

$$\frac{dp(\alpha)}{d\alpha} = \frac{\phi(\alpha)}{\left(5\omega^4 - 3A_3(\alpha_{[Hc]})\omega^2 + A_1(\alpha_{[Hc]})\right)^2 + \left(4A_4(\alpha_{[Hc]})\omega^3 - 2A_2(\alpha_{[Hc]})\omega\right)^2},$$

where $\phi(\alpha) = \big(4A_4(\alpha_{[Hc]})\omega^3 - 2A_2(\alpha_{[Hc]})\omega\big)\big(-A_3'(\alpha_{[Hc]})\omega^3 + A_1'(\alpha_{[Hc]})\omega\big) - \big(5\omega^4 - 3A_3(\alpha_{[Hc]})\omega^2 + A_1(\alpha_{[Hc]})\big)\big(A_4'(\alpha_{[Hc]})\omega^4 - A_2'(\alpha_{[Hc]})\omega^2 + A_0'(\alpha_{[Hc]})\big)$.

Therefore, if the transversality condition holds, i.e.,

$$\left[\frac{d}{d\alpha}\big(Re(\lambda(\alpha))\big)\right]_{\alpha=\alpha_{[Hc]}} = \left[\frac{dp(\alpha)}{d\alpha}\right]_{\alpha=\alpha_{[Hc]}} \neq 0,$$

then the system (4) undergoes a Hopf bifurcation around E_c. ■

In Fig. 8, the coexisting steady state E_c undergoes a Hopf bifurcation with $p_{10} = 0.51$, $p_{20} = 0.85$ and $p_{30} = 0.98$, and induced an unstable limit cycle around E_c.

3.4 Bi-stability of equilibria

Based on the results in the system (3), there exists a mono-stability. When this system is imposed by the immune response, there appears bi-stability, i.e., the healthy and coexisting equilibria E_h and E_c are stable. When the proliferation rate of haematopoietic cells is smaller than the rate of leukaemia cells with a proper immune response, there will be a stable coexisting equilibrium and a stable healthy equilibrium, see Fig. 9. Comparatively, the stable E_h is more robust than the stable E_c because of a bigger attraction basin of E_h. In a word, the introduction of immune response would provide a clear guide to the treatment of AML.

4 Effects of time delays

In this section, we study transcritical and Hopf bifurcations of the delayed system (5), compare the corresponding bifurcations with non-delayed system (4) and explore the effects of time delays on the dynamics.

4.1 The characteristic equation of delayed model

The system (5) are rewritten in the matrix form, that is,

$$\frac{d}{dt}\begin{pmatrix} S \\ A \\ D \\ L \\ T \end{pmatrix} = C_0\begin{pmatrix} S(t) \\ A(t) \\ D(t) \\ L(t) \\ T(t) \end{pmatrix} + C_1\begin{pmatrix} S(t-\tau_1) \\ A(t-\tau_1) \\ D(t-\tau_1) \\ L(t-\tau_1) \\ T(t-\tau_1) \end{pmatrix} + C_2\begin{pmatrix} S(t-\tau_2) \\ A(t-\tau_2) \\ D(t-\tau_2) \\ L(t-\tau_2) \\ T(t-\tau_2) \end{pmatrix} + C_3\begin{pmatrix} S(t-\tau_3) \\ A(t-\tau_3) \\ D(t-\tau_3) \\ L(t-\tau_3) \\ T(t-\tau_3) \end{pmatrix},$$

where $C_0 = \{a_{ij}\}, C_1 = \{b_{ij}\}, C_2 = \{c_{ij}\}, C_3 = \{d_{ij}\}$,

$$C_0|_{E^*} = \begin{pmatrix} f_{1S} & 0 & 0 & 0 & 0 \\ f_{2S} & f_{2A} & 0 & f_{2L} & 0 \\ 0 & f_{3A} & -\mu_D & 0 & 0 \\ 0 & f_{4A} & 0 & a_{44} & 0 \\ 0 & 0 & 0 & f_{5L} & f_{5T} \end{pmatrix},$$

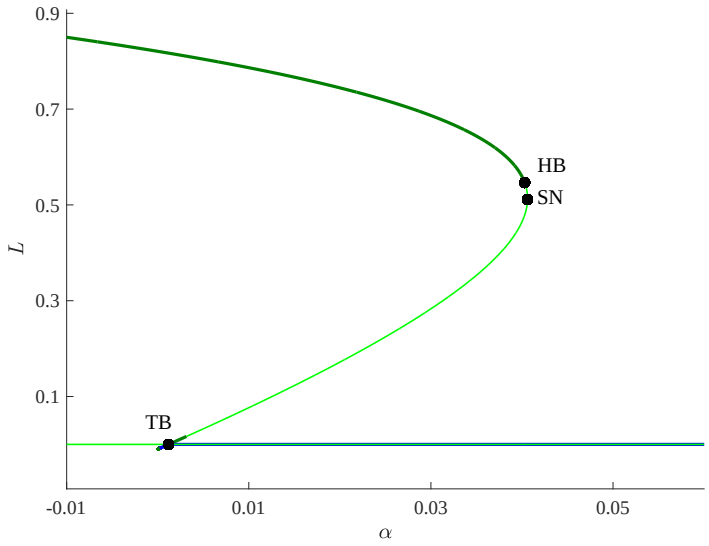

(a) The bifurcation diagram between L and α

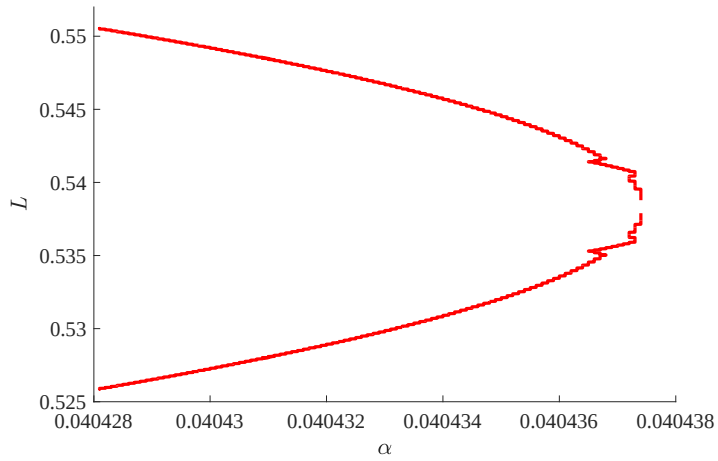

(b) The amplification of the limit cycle induced by the Hopf bifurcation.

Fig. 8 The Hopf bifurcation (HB) diagram between L and α.

and

$$
\begin{aligned}
a_{44} =& \big[p_{30}(2-A-2L)-1\big]v_{30},\\
b_{13} =& f_{1D}, b_{23} = 2S(1-p_1)v_{1D} - 2Sp_{1D}v_1,\\
c_{23} =& \big[p_2(2-A-L)-1\big]v_{2D}A + (2-A-L)p_{2D}v_2A,\\
c_{33} =& 2(1-p_2)v_{2D}A - 2p_{2D}v_2A,\\
d_{44} =& -\frac{\alpha\gamma}{(\gamma+L)^2}.
\end{aligned}
$$

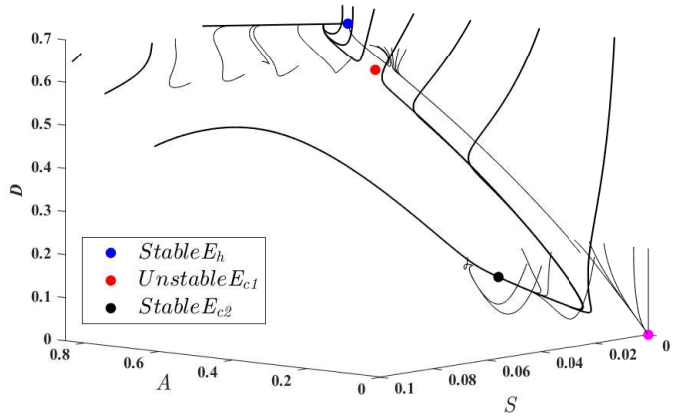

Fig. 9 The diagram (S,A,D) with $p_{10}=0.51$, $p_{20}=0.85$, $p_{30}=0.98$ and $\alpha=0.015$. There is a stable healthy steady state E_h and a stable coexisting steady state E_{c2}.

Then, the characteristic equation of Eq. (5) is

$$\begin{aligned}\Delta_{delay}(\lambda) &= \lambda I-(C_0+e^{-\lambda\tau_1}C_1+e^{-\lambda\tau_2}C_2+e^{-\lambda\tau_3}C_3)\\ &=(\lambda-f_{5T})\Big[(\lambda-f_{1S})\big[(\lambda-f_{2A})(\lambda-c_{33}e^{-\lambda\tau_2}+\mu_D)(\lambda-a_{44}-d_{44}e^{-\lambda\tau_3})\\ &-(b_{23}e^{-\lambda\tau_1}+c_{23}e^{-\lambda\tau_2})f_{3A}(\lambda-a_{44}-d_{44}e^{-\lambda\tau_3})-f_{2L}(\lambda-c_{33}e^{-\lambda\tau_2}+\mu_D)f_{4A}\big]\\ &-(f_{1D}e^{-\lambda\tau_1})f_{2S}f_{3A}(\lambda-a_{44}-d_{44}e^{-\lambda\tau_3})\Big].\end{aligned}\tag{11}$$

To obtain some theoretical results for the time delays, we suppose that $\tau_1=\tau_2=\tau,\tau_3=2\tau$. Then, the characteristic equation (11) is simplified as:

$$\begin{aligned}\Delta_{delay}(\lambda)=&\big(\lambda^5+m_4\lambda^4+m_3\lambda^3+m_2\lambda^2+m_1\lambda+m_0\big)+\big(n_4\lambda^4+n_3\lambda^3+n_2\lambda^2+n_1\lambda+n_0\big)e^{-\lambda\tau}\\ &+\big(p_4\lambda^4+p_3\lambda^3+p_2\lambda^2+p_1\lambda+p_0\big)e^{-2\lambda\tau}+\big(q_3\lambda^3+q_2\lambda^2+q_1\lambda+q_0\big)e^{-3\lambda\tau}.\end{aligned}\tag{12}$$

4.2 Transcritical bifurcation

Firstly, we study the transcritical bifurcation around the purely leukaemia steady state $E_l(0,0,0,L_l^*,T_l^*)$. The characteristic equation (12) becomes

$$\begin{aligned}\Delta(\alpha,E_l,\lambda)=&(\lambda+\mu_D)(\lambda+\mu_T)(\lambda-(2p_{10}-1)v_{10})\times\\ &(\lambda-(p_{20}(2-L_l^*)-1)v_{20})(\lambda-a_{44}(E_l^*)-d_{44}(\alpha)e^{-2\lambda\tau}).\end{aligned}$$

Specifically, the eigenvalues are

$$\lambda_{l1} = (2p_{10}-1)v_{10}, \quad \lambda_{l2} = (p_{20}(2-L_l^*)-1)v_{20}, \quad \lambda_{l3} = -\mu_D,$$
$$\lambda_{l4} = (p_{30}(2-2L_l^*)-1)v_{30} - \frac{\alpha\gamma}{(\gamma+L_l^*)^2}e^{-2\lambda_{l4}\tau}, \quad \lambda_{l5} = -\mu_T.$$

Clearly, the eigenvalue λ_{l4} is related to the time delay, and other eigenvalues are same as the counterparts of non-delayed model. Therefore, it gives the following theorem.

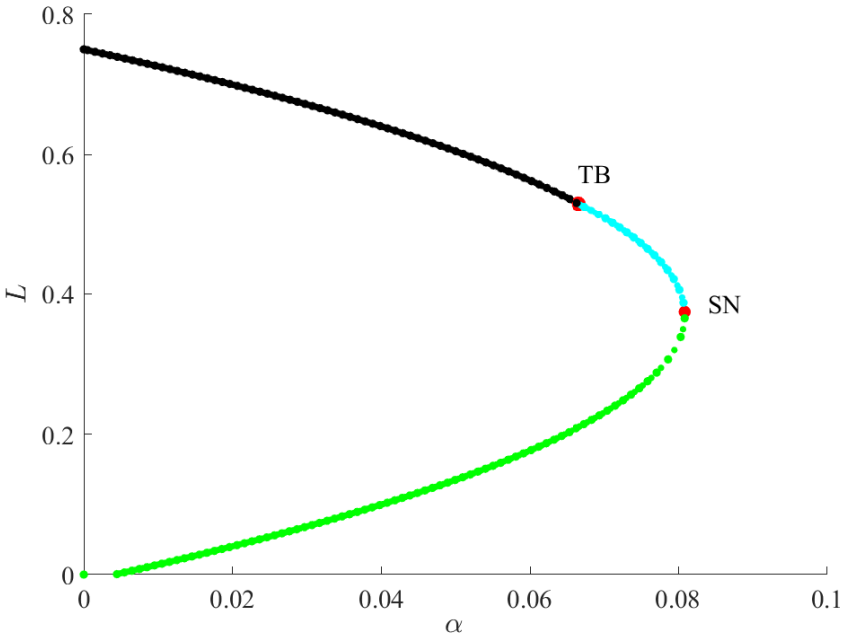

Fig. 10 The bifurcation diagram around the purely leukaemia steady state E_l with $p_{10} = 0.45$ and $\tau = 5$. The transcritical bifurcation point is $\alpha_{[Tl\tau]} = 0.0665$ and the saddle-node bifurcation point is $\alpha_{[SNl\tau]} = 0.08085$. Black dots represent the stable equilibria and cyan and green dots denote the unstable equilibria with one and two positive eigenvalues.

Theorem 8 *The system (5) undergoes a transcritical bifurcation around the state E_l at $\alpha_{[Tl\tau]}$, where $\alpha_{[Tl\tau]}$ is the root of $L_l^*(\alpha) = 2 - \frac{1}{p_{20}}$. It also experiences a transcritical bifurcation around E_h at $\alpha_{[Th\tau]}$, where $\alpha_{[Th\tau]}$ is the root of $\alpha = (p_{30}(2-A_h^*)-1)v_{30}\gamma$.*

Since the transcritical bifurcation takes place around the equilibrium with zero eigenvalues, the critical values of the bifurcation parameter α are not affected by the time delay. Comparing Figs. 10 and 6, Figs. 11 and 7, the delayed system (5) has the same critical values with the non-delayed system (4), which shows that the delays has no effect on the transcritical bifurcation.

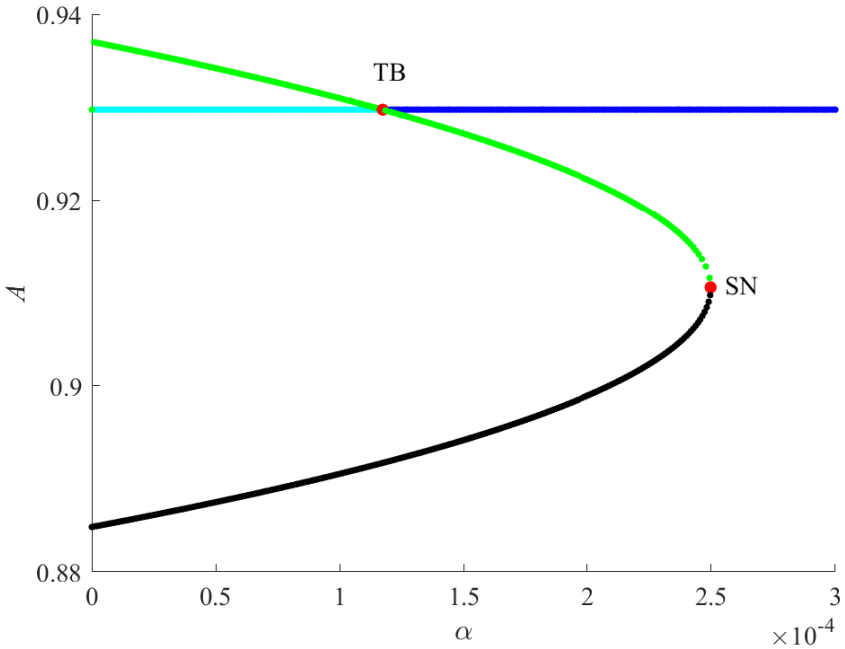

Fig. 11 The bifurcation diagram around the healthy steady state E_h and coexisting steady state E_c with $p_{20} = 0.75$, $p_{30} = 0.95$, $\mu_D = 0.365$ and $\tau = 50$. The saddle-node bifurcation point is $\alpha_{[SNc\tau]} = 0.000249$ and the transcritical bifurcation point is $\alpha_{[Th\tau]} = 0.000117$. Cyan (blue) dots represent the unstable (stable) healthy steady state and green (black) dots denote the unstable (stable) coexisting steady state.

Remark 1 The time delay τ has no effect on the transcritical bifurcation around three types of equilibria in the delayed system (5) with $\tau_1 = \tau_2 = \tau$ and $\tau_3 = 2\tau$.

4.3 Existence of Hopf bifurcation

In this section, we study the existence of Hopf bifurcation around the coexisting steady state E_c and the healthy steady state E_h. Suppose $\lambda = \pm i\omega$ $(\omega > 0)$ is a root of Eq. (12), then it follows

$$\begin{cases} X_1 sin(\omega\tau) + Y_1 cos(\omega\tau) + Z_1 = 0, \\ X_2 sin(\omega\tau) + Y_2 cos(\omega\tau) + Z_2 = 0. \end{cases}$$

Further,

$$\begin{cases} \cos(\omega\tau) = -\dfrac{X_1 Z_2 - X_2 Z_1}{X_1 Y_2 - X_2 Y_1}, \\ \sin(\omega\tau) = -\dfrac{Z_1 Y_2 - Z_2 Y_1}{X_1 Y_2 - X_2 Y_1}, \end{cases}$$

and

$$\begin{aligned} H(v) \equiv H(\omega^2) &= (X_1 Z_2 - X_2 Z_1)^2 + (Y_1 Z_2 - Y_2 Z_1)^2 - (X_1 Y_2 - X_2 Y_1)^2 \\ &= c_{26}\omega^{52} + c_{25}\omega^{50} + \cdots + c_1\omega^2 + c_0. \end{aligned} \tag{13}$$

When the equation $H(v)=0$ has at least one positive root v^*, the characteristic equation (12) has a pair of purely imaginary eigenvalues $\lambda^*=\pm i\omega^*$ with $\omega^*=\sqrt{v^*}$.

Then, the critical delays for the Hopf bifurcation around the steady state E_c are given by

$$\tau_k=\frac{1}{\omega^*}\arccos\left(-\frac{X_1Z_2-X_2Z_1}{X_1Y_2-X_2Y_1}\right)+\frac{2k\pi}{\omega^*},\quad k=0,1,\cdots.$$

Taking the derivative of $\lambda(\tau)$ with respect to τ in Eq. (12) yields

$$\left[\frac{d\lambda(\tau)}{d\tau}\right]^{-1}=\frac{1}{\lambda}\frac{M'+N'e^{-\lambda\tau}+P'e^{-2\lambda\tau}+Q'e^{-3\lambda\tau}}{Ne^{-\lambda\tau}+2Pe^{-2\lambda\tau}+3Qe^{-3\lambda\tau}}-\frac{\tau}{\lambda}. \tag{14}$$

Then, the sign of the real part of Eq. (14) at $\tau=\tau_k$ is

$$\mathrm{sgn}\left[Re\left(\frac{d\lambda(\tau)}{d\tau}\right)^{-1}_{\tau=\tau_k}\right]=\mathrm{sgn}\left[\frac{T_RF_I-T_IF_R}{T_R^2+T_I^2}\right]_{\omega=\omega^*,\tau=\tau_k}.$$

When the transversality condition $T_RF_I-T_IF_R\neq 0$ holds, the system (5) experiences a Hopf bifurcation at the time delays τ_k around the coexisting steady state E_c.

Theorem 9 *For the system (5) with $\tau_1=\tau_2=\tau,\tau_3=2\tau$, we have the following conclusions:*

(i) If the conditions $H_i>0$ $(i=1,\cdots,5)$ hold, the steady states E_c or E_h is locally asymptotically stable for $\tau\in[0,\tau^*)$, $\tau^*=\min_k\{\tau_k\}$.

(ii) If Eq. (13) has at least one positive root and the transversality condition $T_RF_I-T_IF_R\neq 0$ satisfy, the system (5) undergoes a Hopf bifurcation around the steady states E_c or E_h for $\tau=\tau_k$ $(k=0,1,\cdots)$.

Compared to the non-delayed system (4), the delays in the system (5) induce a series of Hopf bifurcations around the healthy steady state E_h, see Fig. 12. Figure 13 shows the time series and the oscillation diagram. The Hopf bifurcation at E_h results in the oscillations of the leukaemia cells and haematopoietic progenitor cells, which means that it is impossible to eliminate all the leukaemia cells. It implies that the stable healthy steady state is just a ideal state, we should focus on the inhibition of the population of the leukaemia cells and try to drive the state of system (5) to a stable limit cycle.

5 Conclusions

In the present study, we have proposed a new acute myeloid leukaemia (AML) model incorporating with feedback regulation, immune response and time delays, which describes the competition between the haematopoietic progenitor cells and the leukaemia stem cells. On the basis of this model, we have shown that the existence and stability of three types of equilibria are determined by the proliferation rates and the strength of immune response. We also have shown that enhancing immunity is an efficient way to prevent and treat the AML. With an increase of the immune response, the leukaemia steady state loses its stability and the healthy steady state becomes stable at different transcritical bifurcation points. When introducing the immune response into the model, it is interesting that the system displays bi-stability feature, which includes both steady states-stable coexisting and healthy steady states when the AML is cured. From the relapse of the AML, the stable healthy steady state

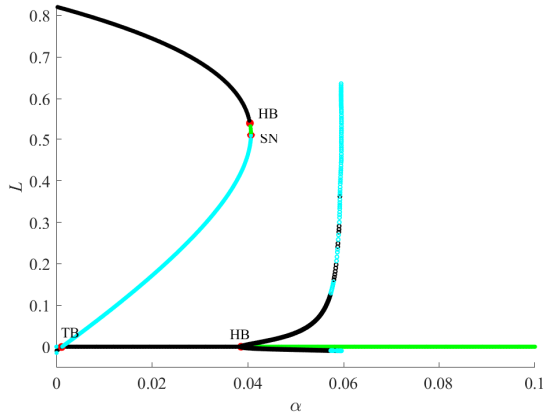

(a) The bifurcation diagram against α with $p_{10} = 0.51$, $p_{20} = 0.85$, $p_{30} = 0.98$ and $\tau = 0.2$.

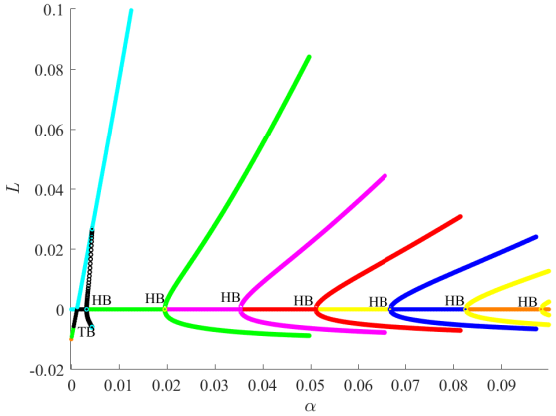

(b) The bifurcation diagram against α with $p_{10} = 0.51$, $p_{20} = 0.85$, $p_{30} = 0.98$ and $\tau = 2$.

Fig. 12 The bifurcation diagrams against α. (a) There exist two Hopf bifurcations around the state E_c and E_h. (b) There is a Hopf bifurcation around E_c and six number of Hopf bifurcations around E_h.

is more robust than the coexisting steady state since the attraction basin of the healthy steady state is bigger.

On the other hand, we have revealed that the time delays have no effect on the transcritical bifurcation around the equilibria. Furthermore, the delays induce a lot of Hopf bifurcations and cause oscillations around the healthy steady state, which means that the leukaemia cells are never eliminated. Analytical results are consistent with the truth that the healthy steady state is an ideal state because there are always normal cells mutate into leukemia cells. From this, we should focus on the inhibition of the population of the leukaemia cells, but not elimination of them. Our main contribution of this paper is that the proposed mathematical model will shed light on the treatments of the AML by changing the immune response and controlling the time delays to drive the states running to the stable coexisting steady state or stable limit cycle around the healthy steady state.

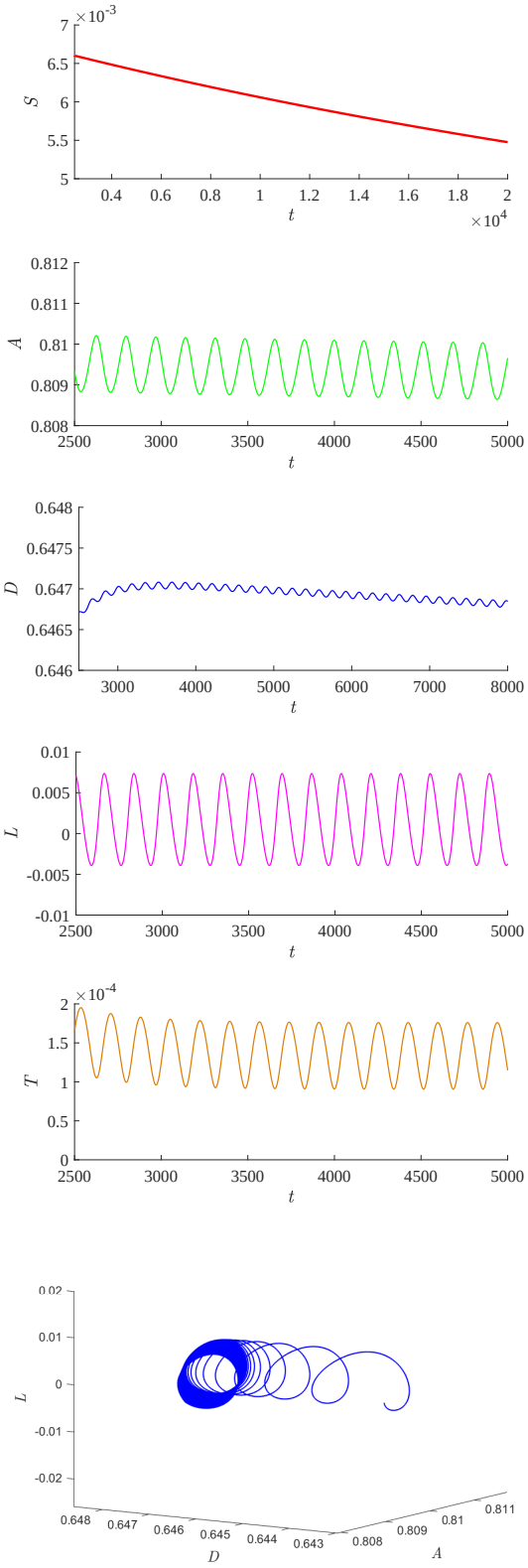

Fig. 13 Time series of S, A, D, L, T and the oscillation diagram of A, D, L induced by the Hopf bifurcation with $\tau = 0.2$.

Data Availability Statement

The datasets generated during and/or analyzed during the current study are available from the corresponding author on reasonable request.

Declarations

Funding This work was supported by the National Natural Science Foundation of China (No. 71932005) and the Zhejiang Provincial Natural Science Foundation of China (No. LY20F030007).

Conflict of interest The authors declare that they have no conflict of interest.

Appendix

A. Numerical Simulations

The non-delayed bifurcation diagrams are performed by Oscill8 software and the delayed bifurcation diagrams are performed by DDE-BIFTOOL, a Matlab toolbox for bifurcation analysis of time-delayed systems, and others are finished by Matlab.

B. Denotations of involved parameters

Table 1: The definitions, basal values and references of all the parameters.

Parameters	Definitions	Basal values	References
p_{10}	The maximal differentiation probability of S	0.65	[25]
p_{20}	The maximal differentiation probability of A	0.68	[25]
p_{30}	The maximal differentiation probability of L	0.80	[25]
v_{10}	The rate of haematopoietic stem cell division	0.50	[25]
v_{20}	The rate of progenitor cell division	0.72	[25]
v_{30}	The rate of leukemogenesis stem cell division	0.70	[28]
μ_D	The rate of D undergoing the apoptosis or death	0.275	[29]
μ_T	The rate of T undergoing the apoptosis or death	0.30	[29]
g_1	The feedback coefficient of S from D	0.03	[24]
g_2	The feedback coefficient of A from D	0.025	[24]
h_1	The feedback coefficient of S from D	0.2	[28]
h_2	The feedback coefficient of S from D	0.11	[28]
α	The characteristic rate of the immune response	0.015	[30]
γ	The half saturation constant of the immune response	0.01	[30]
n	The Hill exponent of $p_1(D), p_2(D)$ and $v_1(D), v_2(D)$	1	[28]
K_1	The carrying capacity of the compartment with S	1	[29]
K_2	The carrying capacity of the compartment with A and L	1	[29]

C. Representations of the parameters

$$
\begin{aligned}
a_0 =& 8v_{10}v_{20}(p_{20}-1)^2(2p_{10}-1)(p_{10}-1)\\
a_1 =& 2(p_{20}-1)v_{20}\big(p_{10}(2p_{20}-1)\mu_D - 4v_{10}(3g_1p_{10}p_{20}+4g_2p_{10}^2-3g_1p_{10}-2g_1p_{20}-6g_2p_{10}+2g_1+2g_2)\big)\\
a_2 =& \mu_D^2 p_{10}p_{20} + 2p_{10}v_{20}(2p_{20}^2(g_1+h_1)-3p_{20}(g_1+g_2+h_1)+g_1+h_1+2g_2)\mu_D\\
&+ 8v_{10}v_{20}(g_1^2(p_{20}^2-2p_{20}+1)+g_1g_2(6p_{10}p_{20}-6p_{10}-4p_{20}+4)+g_2^2(2p_{10}^2-3p_{10}+1))\\
a_3 =& p_{10}p_{20}(g_1+g_2+h_1+h_2)\mu_D^2 - 8g_1g_2v_{10}v_{20}(2g_1p_{20}+3g_2p_{10}-2g_1-2g_2)\\
&- 2p_{10}v_{20}(3g_1g_2p_{20}-2g_1h_1p_{20}^2+3g_1h_1p_{20}+3g_2h_1p_{20}-2g_1g_2-g_1h_1-g_2^2-2g_2h_1)\mu_D\\
a_4 =& p_{10}p_{20}((h_1+h_2)(g_1+g_2)+g_1g_2+h_1h_2)\mu_D^2 + 2g_2p_{10}v_{20}(g_1g_2-3g_1h_1p_{20}+2g_1h_1+g_2h_1)\mu_D\\
&+ 8g_1^2g_2^2v_{10}v_{20}\\
a_5 =& \mu_D^2 p_{10}p_{20}(g_1g_2(h_1+h_2)+h_1h_2(g_1+g_2)) + 2\mu_D g_1g_2^2h_1p_{10}v_{20}\\
a_6 =& p_{10}p_{20}g_1g_2h_1h_2\mu_D^2
\end{aligned}
$$

$$
\begin{aligned}
A_0 =& f_{3A}f_{2D}f_{4L}f_{1S}f_{5T} + f_{4A}f_{3D}f_{2L}f_{1S}f_{5T} - f_{2A}f_{3D}f_{4L}f_{1S}f_{5T} - f_{3A}f_{1D}f_{4L}f_{2S}f_{5T}\\
A_1 =& f_{2A}f_{3D}f_{4L}f_{1S} + f_{3A}f_{1D}f_{4L}f_{2S} - f_{3A}f_{2D}f_{4L}f_{1S} - f_{4A}f_{3D}f_{2L}f_{1S} + f_{2A}f_{3D}f_{4L}f_{5T}\\
&- f_{3A}f_{2D}f_{4L}f_{5T} - f_{4A}f_{3D}f_{2L}f_{5T} + f_{2A}f_{3D}f_{1S}f_{5T} + f_{3A}f_{1D}f_{2S}f_{5T} - f_{3A}f_{2D}f_{1S}f_{5T}\\
&- f_{3A}f_{4L}f_{1S}f_{5T} - f_{4A}f_{2L}f_{1S}f_{5T} + f_{3D}f_{4L}f_{1S}f_{5T}\\
A_2 =& f_{3A}f_{2D}f_{4L} - f_{2A}f_{3D}f_{4L} + f_{4A}f_{3D}f_{2L} - f_{2A}f_{3D}f_{1S} - f_{3A}f_{1D}f_{2S} + f_{3A}f_{2D}f_{1S}\\
&- f_{2A}f_{3D}f_{5T} + f_{3A}f_{2D}f_{5T} - f_{2A}f_{4L}f_{1S} + f_{4A}f_{2L}f_{1S} - f_{2A}f_{4L}f_{5T} + f_{4A}f_{2L}f_{5T}\\
&- f_{3D}f_{4L}f_{1S} - f_{3D}f_{4L}f_{5T} - f_{2A}f_{1S}f_{5T} - f_{3D}f_{1S}f_{5T} - f_{4L}f_{1S}f_{5T}\\
A_3 =& f_{2A}f_{3D} - f_{3A}f_{2D} + f_{2A}f_{4L} - f_{4A}f_{2L} + f_{3D}f_{4L} + f_{1S}f_{2A} + f_{2A}f_{5T} + f_{3D}f_{1S}\\
&+ f_{3D}f_{5T} + f_{4L}f_{1S} + f_{4L}f_{5T} + f_{1S}f_{5T}\\
A_4 =& -f_{1S} - f_{2A} - f_{3D} - f_{4L} - f_{5T}
\end{aligned}
$$

$$
\begin{aligned}
m_0 =& a_{44}\mu_D f_{1S}f_{2A}f_{5T} - \mu_D f_{1S}f_{2L}f_{4A}f_{5T}\\
m_1 =& \mu_D\big(f_{1S}f_{2L}f_{4A} + f_{2L}f_{4A}f_{5T} - f_{1S}f_{2A}f_{5T} - a_{44}f_{1S}f_{5T} - a_{44}f_{2A}f_{5T} - a_{44}f_{1S}f_{2A}\big)\\
&+ a_{44}f_{1S}f_{2A}f_{5T} - f_{1S}f_{2L}f_{4A}f_{5T}\\
m_2 =& -a_{44}\big(f_{1S}f_{2A} + f_{2A}f_{5T} + f_{1S}f_{5T} - f_{2A}\mu_D - f_{1S}\mu_D - f_{5T}\mu_D\big)\\
&- \mu_D\big(f_{2L}f_{4A} - f_{1S}f_{2A} - f_{2A}f_{5T} - f_{1S}f_{5T}\big) + f_{1S}f_{2L}f_{4A} + f_{2L}f_{4A}f_{5T} - f_{1S}f_{2A}f_{5T}\\
m_3 =& a_{44}(f_{1S} + f_{2A} + f_{5T}) - \mu_D(a_{44} + f_{1S} + f_{2A} + f_{5T}) - f_{4A}f_{2L} + f_{1S}f_{2A} + f_{2A}f_{5T} + f_{1S}f_{5T}\\
m_4 =& \mu_D - a_{44} - f_{1S} - f_{2A} - f_{5T}
\end{aligned}
$$

$$
\begin{aligned}
n_0 =& a_{44}b_{23}f_{1S}f_{3A}f_{5T} - a_{44}f_{1D}f_{2S}f_{3A}f_{5T} + c_{33}f_{1S}f_{2L}f_{4A}f_{5T} + a_{44}c_{23}f_{1S}f_{3A}f_{5T} - a_{44}c_{33}f_{1S}f_{2A}f_{5T}\\
n_1 =& -a_{44}b_{23}f_{1S}f_{3A} - a_{44}b_{23}f_{3A}f_{5T} + a_{44}f_{1D}f_{2S}f_{3A} - b_{23}f_{1S}f_{3A}f_{5T} + f_{1D}f_{2S}f_{3A}f_{5T}\\
&- a_{44}c_{23}f_{1S}f_{3A} + a_{44}c_{33}f_{1S}f_{2A} - a_{44}c_{23}f_{3A}f_{5T} + a_{44}c_{33}f_{2A}f_{5T} + a_{44}c_{33}f_{1S}f_{5T}\\
&- c_{33}f_{1S}f_{2L}f_{4A} - c_{33}f_{2L}f_{4A}f_{5T} - c_{23}f_{1S}f_{3A}f_{5T} + c_{33}f_{1S}f_{2A}f_{5T}\\
n_2 =& a_{44}b_{23}f_{3A} + b_{23}f_{1S}f_{3A} + b_{23}f_{3A}f_{5T} - f_{1D}f_{2S}f_{3A} + a_{44}\big(c_{23}f_{3A} - c_{33}f_{2A} - c_{33}f_{1S} - c_{33}f_{5T}\big)\\
&+ c_{33}\big(f_{2L}f_{4A} - f_{1S}f_{2A} - f_{2A}f_{5T} - f_{1S}f_{5T}\big) + c_{23}f_{3A}f_{1S} + c_{23}f_{3A}f_{5T}\\
n_3 =& -(c_{23} + b_{23})f_{3A} + c_{33}\big(a_{44} + f_{2A} + f_{1S} + f_{5T}\big)\\
n_4 =& -c_{33}
\end{aligned}
$$

$$
\begin{aligned}
p_0 =& d_{44}\mu_D f_{1S}f_{2A}f_{5T}\\
p_1 =& d_{44}\big(f_{1S}f_{2A}f_{5T} - \mu_D f_{1S}f_{2A} - \mu_D f_{2A}f_{5T} - \mu_D f_{1S}f_{5T}\big)\\
p_2 =& -d_{44}\big(f_{1S}f_{2A} + f_{2A}f_{5T} + f_{1S}f_{5T} - f_{2A}\mu_D - f_{1S}\mu_D - f_{5T}\mu_D\big)\\
p_3 =& d_{44}\big(f_{1S} + f_{2A} + f_{5T} - \mu_D\big)\\
p_4 =& -d_{44}
\end{aligned}
$$

$$
\begin{aligned}
q_0 =& d_{44}\big(b_{23}f_{1S}f_{3A}f_{5T} - f_{1D}f_{2S}f_{3A}f_{5T} + c_{23}f_{1S}f_{3A}f_{5T} - c_{33}f_{1S}f_{2A}f_{5T}\big)\\
q_1 =& d_{44}\big(-b_{23}f_{1S}f_{3A} - b_{23}f_{3A}f_{5T} + f_{1D}f_{2S}f_{3A} + c_{33}f_{1S}f_{2A}\\
&- c_{23}f_{1S}f_{3A} - c_{23}f_{3A}f_{5T} + c_{33}f_{2A}f_{5T} + c_{33}f_{1S}f_{5T}\big)\\
q_2 =& -d_{44}\big(c_{33}f_{1S} + c_{33}f_{2A} + c_{33}f_{5T} - c_{23}f_{3A} - b_{23}f_{3A}\big)\\
q_3 =& c_{33}d_{44}
\end{aligned}
$$

$$
\begin{aligned}
M_R =& m_4\omega^4 - m_2\omega^2 + m_0, M_I = \omega^5 - m_3\omega^3 + m_1\omega \\
N_R =& n_4\omega^4 - n_2\omega^2 + n_0, N_I = -n_3\omega^3 + n_1\omega \\
P_R =& p_4\omega^4 - p_2\omega^2 + p_0, P_I = -p_3\omega^3 + p_1\omega \\
Q_R =& -q_2\omega^2 + q_0, Q_I = -q_3\omega^3 + q_1\omega
\end{aligned}
$$

$$
\begin{aligned}
X_1 =& (M_IQ_I - M_RQ_R)(P_I - M_I) - (M_RQ_I + M_IQ_R)(M_R - P_R) + (Q_R^2 + Q_I^2)(Q_I - N_I) \\
Y_1 =& (M_IQ_I - M_RQ_R)(M_R + P_R) - (M_RQ_I + M_IQ_R)(M_I + P_I) + (Q_R^2 + Q_I^2)(N_R + Q_R) \\
Z_1 =& (M_IQ_I - M_RQ_R)N_R - (M_RQ_I + M_IQ_R)N_I + (Q_R^2 + Q_I^2)P_R \\
X_2 =& (M_RQ_R - M_IQ_I)(M_R - P_R) - (M_RQ_I + M_IQ_R)(P_I - M_I) + (Q_R^2 + Q_I^2)(N_R - Q_R) \\
Y_2 =& (M_RQ_R - M_IQ_I)(M_I + P_I) - (M_RQ_I + M_IQ_R)(M_R + P_R) + (Q_R^2 + Q_I^2)(N_I + Q_I) \\
Z_2 =& (M_RQ_R - M_IQ_I)N_I - (M_RQ_I + M_IQ_R)N_R + (Q_R^2 + Q_I^2)P_I
\end{aligned}
$$

$$
\begin{aligned}
M =& \lambda^5 + m_4\lambda^4 + m_3\lambda^3 + m_2\lambda^2 + m_1\lambda + m_0 \\
N =& n_4\lambda^4 + n_3\lambda^3 + n_2\lambda^2 + n_1\lambda + n_0 \\
P =& p_4\lambda^4 + p_3\lambda^3 + p_2\lambda^2 + p_1\lambda + p_0 \\
Q =& q_3\lambda^3 + q_2\lambda^2 + q_1\lambda + q_0
\end{aligned}
$$

$$
\begin{aligned}
M' =& 5\lambda^4 + 4m_4\lambda^3 + 3m_3\lambda^2 + 2m_2\lambda + m_1 \\
N' =& 4n_4\lambda^3 + 3n_3\lambda^2 + 2n_2\lambda + n_1 \\
P' =& 4p_4\lambda^3 + 3p_3\lambda^2 + 2p_2\lambda + p_1 \\
Q' =& 3q_3\lambda^2 + 2q_2\lambda + q_1 \\
F_R =& M_R' + N_R'\cos(\omega\tau) + N_I'\sin(\omega\tau) + P_R'\cos(2\omega\tau) + P_I'\sin(2\omega\tau) + Q_R'\cos(3\omega\tau) + Q_I'\sin(3\omega\tau)
\end{aligned}
$$

$$
\begin{aligned}
F_I =& M_I' + N_I'\cos(\omega\tau) - N_R'\sin(\omega\tau) + P_I'\cos(2\omega\tau) - P_R'\sin(2\omega\tau) + Q_I'\cos(3\omega\tau) - Q_R'\sin(3\omega\tau) \\
T_R =& N_R\cos(\omega\tau) + N_I\sin(\omega\tau) + 2P_R\cos(2\omega\tau) + 2P_I\sin(2\omega\tau) + 3Q_R\cos(3\omega\tau) + 3Q_I\sin(3\omega\tau) \\
T_I =& N_I\cos(\omega\tau) - N_R\sin(\omega\tau) + 2P_I\cos(2\omega\tau) - 2P_R\sin(2\omega\tau) + 3Q_I\cos(3\omega\tau) - 3Q_R\sin(3\omega\tau)
\end{aligned}
$$

References

1. Estey, E., Döhner, H.: Acute myeloid leukaemia. Lancet **368**, 1894-1907 (2006)
2. Khwaja, A., Bjorkholm, M., Gale, R., Levine, R., Jordan, C.: Acute myeloid leukaemia. Nat. Rev. Dis. Primers **2**, 16010 (2016)
3. Lapidot, T., Sirard, C., Vormoor, J., Murdoch, B., Hoang, T., Caceres, C., Minden, M., Paterson, B., Caligiuri, M., Dick, J.: A cell initiating human acute myeloid leukaemia after transplantation into SCID mice. Nature **367**, 645-648 (1994)
4. Bonnet, D., Dick, J.: Human acute myeloid leukemia is organized as a hierarchy that originates from a primitive hematopoietic cell. Nat. Med. **3**, 730-737 (1997)
5. Passegué, E., Jamieson, C., Ailles, L., Weissman, I.: Normal and leukemic hematopoiesis: are leukemias a stem cell disorder or a reacquisition of stem cell characteristics. Proc. Natl. Acad. Sci. **100**, 11842-11849 (2003)

6. Döhner, H., Estey, E., Amadori, S., et al.: Diagnosis and management of acute myeloid leukemia in adults: recommendations from an international expert panel on behalf of the European LeukemiaNet. Blood **115**, 453-474 (2010)
7. Linker, C.: Autologous stem cell transplantation for acute myeloid leukemia. Bone Marrow Transplant. **31**, 731-738 (2003)
8. Schuurhuis, G., Meel, M., Wouters, F., Min, L. et al.: Normal hematopoietic stem cells within the AML bone marrow have a distinct and higher ALDH activity level than co-existing leukemic stem cells. Plos One **8**, e78897 (2013)
9. Saito, Y., Uchida, N., Tanaka, S., Suzuki, N. et al.: Induction of cell cycle entry eliminates human leukemia stem cells in a mouse model of AML. Nat. Biotechnol. **28**, 275-280 (2010)
10. Andersen, L., Mackey, M.: Resonance in periodic chemotherapy: a case study of acute myelogenous leukemia. J. Theor. Biol. **209**, 113-130 (2001)
11. Dean, M., Fojo, T., Bates, S.: Tumour stem cells and drug resistance. Net. Rev. Cancer **5**, 275-284 (2005)
12. Roeder, I., Loeffler, M.: A novel dynamic model of hematopoietic stem cell organization based on the concept of within-tissue plasticity. Exp. Hematol. **30** , 853-861 (2002)
13. Liso, A., Castiglione, F., Cappuccio, A., Stracci, F., Schlenk, R., Amadori, S. et al.: A one-mutation mathematical model can explain the age incidence of acute myeloid leukemia with mutated nucleophosmin (NPM1). Haematologica **93**, 1219-1226 (2008)
14. Cucuianu, A., Precup, R.: A hypothetical-mathematical model of acute myeloid leukaemia pathogenesis. Comput. Math. Methods Med. **11**, 49-65 (2010)
15. Tan, B., Park, C., Ailles, L., Weissman, I.: The cancer stem cell hypothesis: a work in progress. Lab. Invest. **86**, 17075578 (2006)
16. Stiehl, T., Baran, N., Ho, A., Marciniak, C.: Clonal selection and therapy resistance in acute leukaemias: mathematical modelling explains different proliferation patterns at diagnosis and relapse. J. R. Soc. Interface **11**, 20140079 (2014)
17. Stiehl, T., Baran, N., Ho, A., Marciniak, C.: Cell division patterns in acute myeloid leukemia stem-like cells determine clinical course: a model to predict patient survival. Cancer Res. **75**, 940-949 (2015)
18. Stiehl, T., Marciniak, C.: Mathematical modeling of leukemogenesis and cancer stem cell dynamics. Math. Model. Nat. Phenom. **7**, 166-202 (2012)
19. MacLean, A., Filippi, S., Stumpf, M.: The ecology in the hematopoietic stem cell niche determines the clinical outcome in chronic myeloid leukemia. Proc. Natl. Acad. Sci. **111**, 3882-3888 (2014)
20. Cozzio, A., Passegué, E., Ayton, P., Karsunky, H., Cleary, M., Weissman, I.: Similar MLL-associated leukemias arising from self-renewing stem cells and short-lived myeloid progenitors. Genes Dev. **17**, 3029-3035 (2003)
21. Goardon, N., Marchi, E., Atzberger, A., Quek, L., Schuh, A., Soneji, S., Woll, P., Mead, A. et al.: Coexistence of LMPP-like and GMP-like leukemia stem cells in a cute myeloid leukemia. Cancer Cell **19**, 138-152 (2011)
22. Leo, D., Wagers, A.: Dynamic niches in the origination and differentiation of haematopoietic stem cells. Nat. Rev. Mol. Cell Biol. **12**, 643-655 (2011)
23. Marciniak, C., Stiehl, T., Ho, A., Jäger, W., Wagner, W.: Modeling of asymmetric cell division in hematopoietic stem cells-regulation of self-renewal is essential for efficient repopulation. Stem Cells Dev. **18**, 377-385 (2009)
24. Lo, W., Chou, C., Gokoffski, K., Wan, F., Lander, A., Calof, A., Nie, Q.: Feedback regulation in multistage cell lineages. Math. Biosci. Eng. **6**, 59-82 (2009)
25. Ignacio, A., Brenesa, R., Natalia, L., Wodarz, D.: Evolutionary dynamics of feedback escape and the development of stem-cell-driven cancers. Proc. Natl. Acad. Sci. **108**, 18983-18988 (2011)
26. Lander, A., Gokoffski, K., Wan, F., Nie, Q., Calof, A.: Cell lineages and the logic of proliferative control. Plos Biol. **7**, 84-100 (2009)
27. Pirayesh, B., Pazirandeh, A., Akbari, M.: Local bifurcation analysis in nuclear reactor dynamics by Sotomayor's theorem. Ann. Nucl. Energy **94**, 716731 (2016)
28. Crowell, H., MacLean, A., Stumpf, M.: Feedback mechanisms control coexistence in a stem cell model of acute myeloid leukaemia. J. Theor. Biol. **401**, 43-53 (2016)
29. Jiao, J., Luo, M., Wang, R.: Feedback regulation in a stem cell model with acute myeloid leukaemia. BMC Syst. Biol. **12**, 75-83 (2018)
30. Sharp, J., Browning, A., Mapder, T., Burrage, K., Simpson, M.: Optimal control of acute myeloid leukaemia. J. Theor. Biol. **470**, 30-42 (2019)
31. Qi, A., Beretta, E., Kuang, Y., Wang, C., Wang, H.: Geometric stability switch criteria in delay differential equations with two delays and delay dependent parameters. Electron **266**, 7073-7100 (2019)
32. Austina, R., Smythab, M., Lane, S.: Harnessing the immune system in acute myeloid leukaemia. Crit. Rev. Oncol. **103**, 62-77 (2016)

33. Song, Z., Wang, C., Zhen, B.: Codimension-two bifurcation and multistability coexistence in an inertial two-neuron system with multiple delays. Nonlinear Dyn. **85**, 2099-2113 (2016)
34. Kim, P., Gu, K., Lee, P., Levy, D.: Stability crossing boundaries of delay systems modeling immune dynamics in leukemia. Discrete Cont. Dyn. A **13** 129-156 (2010)
35. Yang, L., Sun, W., Turcotte, M.: Coexistence of hopf-born rotation and heteroclinic cycling in a time-delayed three-gene auto-regulated and mutually-repressed core genetic regulation network. J. Theor. Biol. **27**, 110831 (2021)
36. Yao, H., Price, T., Cantelli, G., Ngo, B., Warner, M., Olivere, L., Ridge, S.: Leukaemia hijacks a neural mechanism to invade the central nervous system. Nature **560**, 55-60 (2018)
37. Pirayesh, B., Pazirandeh, A., Akbari, M.: Local bifurcation analysis in nuclear reactor dynamics by Sotomayor's theorem. Ann. Nucl. Energy **94**, 716-731 (2016)